Preparation of Ultraviolet-Cured Bisphenol A Epoxy Diacrylate/Montmorillonite Nanocomposites with a Bifunctional, Reactive, Organically Modified Montmorillonite as the Only Initiator via *In Situ* Polymerization

Yangling Zang,[1] Weijian Xu,[1] Guangpeng Liu,[1] Deyue Qiu,[2] Shengpei Su[2]

[1]*College of Chemistry and Chemical Engineering, Hunan University, Changsha 410082, China*
[2]*College of Chemistry and Chemical Engineering, Hunan Normal University, Changsha 410081, China*

Received 16 February 2008; accepted 4 August 2008
DOI 10.1002/app.29134
Published online 13 October 2008 in Wiley InterScience (www.interscience.wiley.com).

ABSTRACT: A bifunctional reactive surfactant containing a polymerizable methacrylate group and a benzophenone group, [2-(methacryloyloxy)ethyl](4-benzoylbenzyl)dimethylammonium bromide (MDAB), was synthesized to modify montmorillonite (MMT) for the preparation of nanocomposites via photoinduced polymerization. Fourier transform infrared, thermogravimetric analysis, and X-ray diffraction results indicated that MDAB-modified MMT was obtained and had intercalated structures. The morphology of the ultraviolet-cured bisphenol A epoxy diacrylate/MMT nanocomposites prepared from the organically modified MMTs was studied with X-ray diffraction and transmission electron microscopy, and the results showed an intercalated structure with partial exfoliation for all the samples. Experimental results from thermogravimetric analysis, differential scanning calorimetry, and mechanical property testing also indicated that the thermal and mechanical properties of the ultraviolet-cured nanocomposites were significantly enhanced by the presence of this bifunctional, reactive, organically modified MMT. © 2008 Wiley Periodicals, Inc. J Appl Polym Sci 111: 813–818, 2009

Key words: curing of polymers; organoclay; photopolymerization

INTRODUCTION

Ultraviolet (UV)-induced curing technology has been used in various areas and especially in the electronics industry because of its high efficiency, environmental friendliness, and energy savings.[1–3] However, in some cases such as printed circuits, patterning (video disks), sealants (encapsulation), and conformal coatings, it is necessary to prepare a polymer film with a high glass-transition temperature (T_g), good barrier properties, low shrinkage, remarkable flexibility, enhanced mechanical properties, thermal stability, and chemical resistance. Fortunately, most of the requirements can be satisfied with the application of clay nanotechnology. We know that a lot of polymer properties, including those mentioned, can be greatly enhanced even with a low loading of clays.[4–7] Therefore, it is not a surprise that UV-curable clay nanocomposites, which combine the advantages of both UV curing and nanotechnology, have attracted so much attention in recent years since Zahouily et al.[8] first reported their preparation of UV-curable polymer–clay nanocomposites.

In general, montmorillonite (MMT) is organically modified to achieve the exfoliation of the silicate platelets and compatibility between the clay and polymer or monomer in the preparation of nanocomposites.[9–12] Surfactants with reactive groups such as acrylic and styrene groups have been employed to modify clays to improve the compatibility between the clay and polymer matrix through the C=C bonds participating in the polymerization that follows.[13–18] Keller et al.[15] described a method in which reactive acrylate-modified nanoclays were dispersed in UV-cured urethane acrylate, and the tensile strength and elongation at break of the UV-cured nanocomposites were greatly improved in comparison with a microcomposite prepared from unmodified clay. To expand their research on the compatibility between clays and polymer matrices, Dean et al.,[16] using both ion exchange and silane

Correspondence to: S. Su (sushengpei@gmail.com).
Contract grant sponsor: Hunan Provincial Nature Science Foundation; contract grant number: 08JJ4005.
Contract grant sponsor: Xiaoxiang Scholar Foundation, Hunan Normal University; contract grant number: 050613.

© 2008 Wiley Periodicals, Inc.

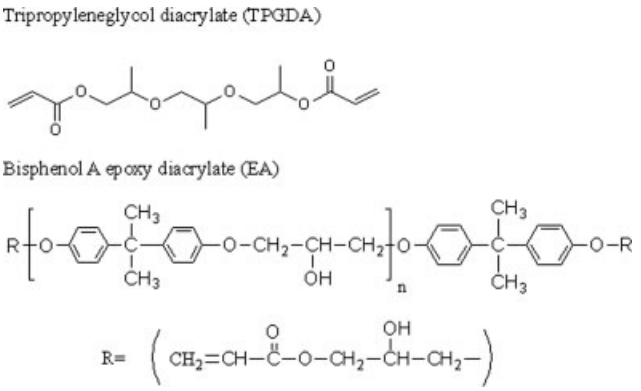

Figure 1 Chemical structures of the components in the UV-curable resins.

grafting chemistry, prepared four UV-active clays that contained either acrylate or methacrylate groups capable of reactions with acrylate groups in the urethane acrylate matrix. X-ray diffraction (XRD) results and transmission electron microscopy (TEM) images showed a predominantly intercalated structure with partial exfoliation in the nanocomposites. Wang and Hsieh[17] reported an unusual geometrical surfactant with a reactive methacrylic group (GME-N-C_{10}) used to effectively expand the lamellar spacing of clays in the preparation of organically modified clays; Uhl and coworkers[13,19] first proposed the concept of using a novel benzophenone surfactant containing acrylate functional groups to modify clays. Their experimental results indicated that the UV-cured urethane acrylate/MMT nanocomposites prepared with this novel organically modified clay had intercalated or exfoliated structures. However, there is no report about a polymerizable, cationic-photoinitiator-modified MMT as the only photoinitiator in UV-cured bisphenol A epoxy diacrylate (EA)/MMT nanocomposites.

In this work, we prepared a polymerizable, photoinitiator-modified MMT with a bifunctional, reactive surfactant containing methacrylate and benzophenone groups, and it was the only photoinitiator in the preparation of UV-cured EA/MMT nanocomposites. We expected polymerization to occur on the clay and an enhancement of the compatibility of the clay with the polymer matrix to be obtained.

EXPERIMENTAL

Materials

EA, purchased from Sartomer Co. (Exton, PA), was used as a telechelic oligomer, the reactive diluent, tripropyleneglycol diacrylate (TPGDA), was provided by UCB Co. (Shanghai, China) and their structure is shown in Figure 1. Pristine sodium montmorillonite (Na-MMT) was provided by Zhejiang Fenghong Clay Chemicals Co., Ltd. (Hangzhow, China) (cation-exchange concentration = 90 mequiv/100 g).

Synthesis of [2-(methacryloyloxy)ethyl](4-benzoylbenzyl)dimethylammonium bromide (MDAB)

The title compound was prepared by the reaction of dimethylaminoethylmetharylate with 4-bromomethyl benzophenone (molar ratio = 1 : 1) in acetone at 55°C for 8 h, and the reaction is described in Figure 2. The crude product was then recrystallized from acetone. After being dried *in vacuo* at room temperature, the purified MDAB was obtained as white crystals.

mp: 156–157°C.[20] ^{1}H-NMR ($CDCl_3$, δ): 7.27–7.95 (m, 9H), 6.13 (s, 1H), 5.64 (s, 1H), 5.41 (s, 2H), 4.74–4.75 (m, 2H), 4.25–4.26 (t, 2H), 3.46 (s, 6H), 1.92 (s, 3H).

Preparation of MDAB-modified MMT [organically modified montmorillonite (OMMT)]

Na-MMT (50 g) was suspended in 10 L of a distilled water–methanol solution (water/methanol = 5/6 v/v) and stirred overnight. To this stirred clay suspension, a solution of MDAB [21 g of MDAB in 600 mL of a water–methanol solution (water/methanol = 5/6 v/v)] was added dropwise. After the solution was stirred for another 10 h at room temperature, the precipitate was filtered and washed repeatedly with a water–methanol solution (water/methanol = 5/6 v/v) until no bromide ion could be detected by an acidic aqueous $AgNO_3$ solution and no MDAB was detected by HPLC. After being dried at 40°C *in vacuo* overnight, this organically modified clay was ground into a powder with a particle size of less than 45 μm. Thermogravimetric analysis (TGA) of this obtained OMMT indicated an organic content of 18 wt %.

Preparation of the EA/MMT UV-cured nanocomposites

A comparative experimental study on the properties of clay nanocomposites was performed. In one case, OMMT was used as the only photoinitiator in the UV-curable formulation, and the clay loadings in this system were varied from 1 to 5 wt %. In the other case, 1 wt % MDAB was added as the

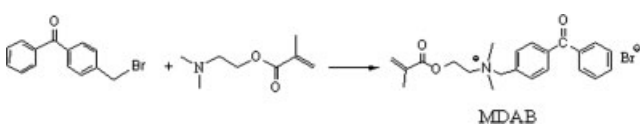

Figure 2 Scheme for the synthesis of the bifunctional photoinitiator MDAB.

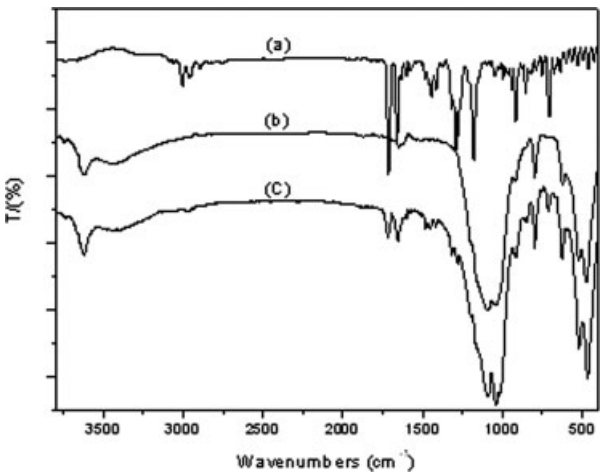

Figure 3 FTIR spectra obtained from (a) MDAB, (b) Na-MMT, and (c) OMMT.

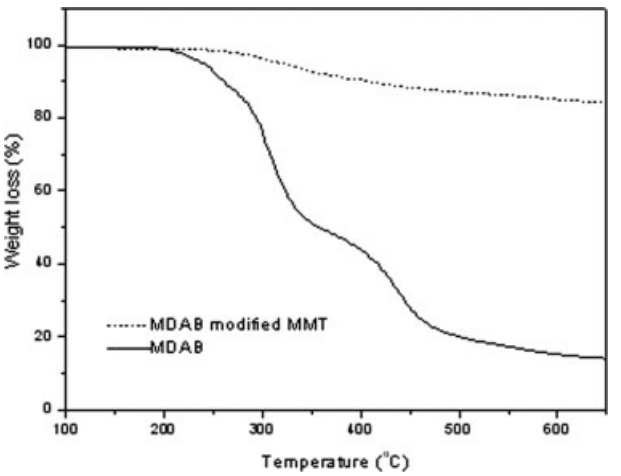

Figure 4 TGA traces obtained for MDAB and OMMT.

photoinitiator, and the loadings of pristine clay were varied from 0 to 3 wt %. In a typical process, the reactive diluent TPGDA was added to EA, and this mixture was stirred for 2 h. After the resin was dispersed, the calculated amount of MDAB and clay (or OMMT) was added to the mixture. This mixture was then homogenized with a high-speed emulsifier at 30°C for 2 h, and this was followed by sonication for 8 h. Finally, the homogenized mixture was degassed *in vacuo* to remove the entrapped air. To avoid premature polymerization caused by the light, the samples were wrapped in aluminum foil for the whole process. The obtained resin was poured into a rectangular organic glass mold (150 mm × 50 mm × 2 mm) with two removable glass slides, which were lined with poly(ethylene terephthalate) films to allow easy removal of the samples after photocuring. The samples were exposed to the UV radiation from a high-pressure mercury lamp (output power = 600 W/cm^2). The incident light intensity at the sample position was measured by radiometry to be 400 W/cm^2. A shutter was used to allow accurate control of the exposure time of the sample by the light. All samples were exposed to the UV lamp for 2 min (1 min on each side) at the ambient temperature.

Instrumentation

^{1}H-NMR spectra were collected on a Varian (Palo Alto, CA) Inova 300 FT-NMR spectrometer with $CDCl_3$ as the solvent. Infrared spectroscopy analysis was performed on a WQF-200 instrument (Beijing, China) with conventional KBr pellets. A mixture of 1 mg of the sample powder with 100 mg of dried KBr crystals was pressed into a 13-mm-diameter pellet. TGA was performed on a Netzsch (Bavaria, Germany) STA409PC instrument under a flowing nitrogen atmosphere from 30 to 700°C at a scan rate of 20°C/min. All TGA results were the averages of a minimum of three determinations; the temperatures were reproducible to ±3°C, whereas the error bars on the fraction of the nonvolatile material was ±3%. Differential scanning calorimetry (DSC) was performed on a TA Instruments (New Castle, DE) Q 20 series calorimeter. Samples were subjected to a heat–cool–heat cycle from −20 to 200°C at a ramp rate of 10°C/min. T_g values were determined as the midpoint of the inflection from the second heat cycle. XRD patterns were collected from 0.5 to 10° with a scan time of 10 s/step with a Bruker (Karlsruhe, Germany) D8 instrument with a step size of 0.1°. Cu Kα X-ray radiation and a random powder mount were used. TEM images of the composites were obtained at 80 kV with a JEOL-1230 (Tokyo, Japan). The samples were ultramicrotomed with a diamond knife at room temperature to give sections approximately 50 nm thick. The sections were transferred from the knife edge to 600-mesh hexagonal Cu grids. The tensile tests were performed at room temperature

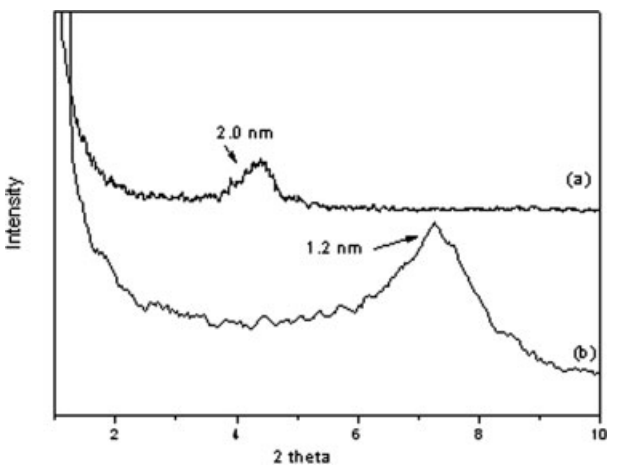

Figure 5 XRD traces obtained from (a) OMMT and (b) Na-MMT.

TABLE I
Cure Times of the UV-Cured Composites for Complete Conversion

	EA/MMT	EA/MMT	EA/OMMT	EA/OMMT	EA/OMMT
Clay weight (%)	0	3	1	3	5
Initiator weight (%)	1	1	0.24	0.72	1.2
Cure time (s)	12	12	21	16	14

with a WDW (Chengde, China) 3020 Instron universal testing machine with a constant crosshead speed of 0.2 in/min; the reported values were the averages of five determinations.

RESULTS AND DISCUSSION

Structure and thermal stability of the modified clay

Fourier transform infrared (FTIR) spectra

Typical FTIR spectra of MMT, MDAB, and OMMT are shown in Figure 3. Two new absorbance bands are present in the FTIR spectrum of OMMT in addition to the typical bands for the pristine clay. These absorbance bands include a band at 1720 cm^{-1}, which can be attributed to the C=O stretching of the carbonyl group, and a band at 1660 cm^{-1}, which can be attributed to C=C stretching. Both of these bands are characteristic FTIR absorbance bands for MDAB. This evidence indicates that MDAB-modified clay (OMMT) was obtained.

TGA characterization

The thermal degradation behaviors of OMMT and MDAB are graphically shown in Figure 4. It is obvious that there are two degradation steps at 200 and 350°C for MDAB. The initial degradation at about 200°C is attributable to a Hoffman degradation mechanism of the quaternary ammonium salts.[21] For OMMT, the initial degradation temperature is 250°C, which indicates higher thermal stability versus MDAB.

XRD results

XRD patterns are shown in Figure 5. The peak at $2\theta = 7.0°$ corresponds to a *d*-spacing of 1.2 nm for the pristine clay, and the peak at $2\theta = 4.4°$ corresponds to a *d*-spacing of 2.0 nm for OMMT. This increase in the *d*-spacing (0.8 nm) is due to the incorporation of the bifunctional, reactive surfactant MDAB and indicates that an intercalated structure of OMMT has been obtained.

Preparation, morphology, and properties of the EA/MMT UV-cured nanocomposites

Cure time of UV-cured intragallery polymerization

In general, *cure* refers to the crosslinking of a polymer to produce a three-dimensional network, and the observed phenomenon includes a change in the refractive index or tackiness in the cure process. In this experiment, the time for the formation of a tack-free film was taken as the cure time for complete conversion. The cure times for both OMMT and pristine clay/MDAB systems are listed in Table I. These experimental data indicate that the cure time is not significantly affected by the presence of clay in the pristine clay/MDAB system.[14,16] However, the situation for the OMMT system is different: the anchored photoinitiator acts as the only initiator in the cure process, and it takes a longer time to cure completely even though it has been calculated that more initiator is used. A reasonable account is that the photoinitiator is anchored to the gallery of the clay, and the intensity of the UV radiation acting on the photoinitiator is reduced; this leads to a slower cure process of the acrylate. At the same time, a reduced cure time is observed when the amount of OMMT in the OMMT system is increased.

XRD and TEM results

The XRD patterns of OMMT and its nanocomposites at different clay loadings are shown in Figure 6. The XRD pattern for OMMT indicates that the clay displacement has been enlarged to 2.0 nm, corresponding to a 2θ value of 4.4°, because of the intercalation of photoinitiator molecules in the clay galleries.

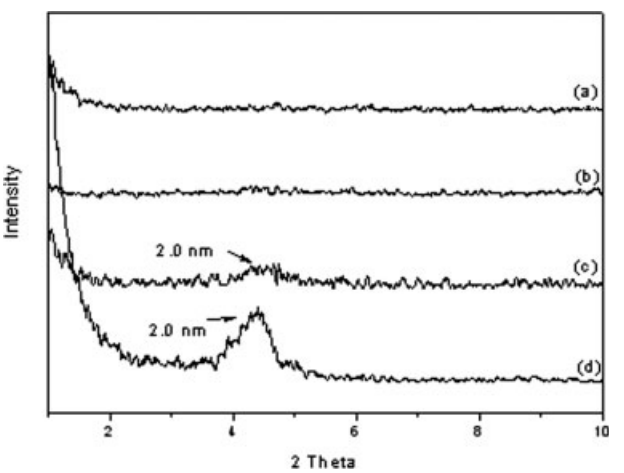

Figure 6 XRD traces obtained from (d) OMMT and (a–c) UV-cured EA/OMMT nanocomposites with clay loadings of 1, 3, and 5%, respectively.

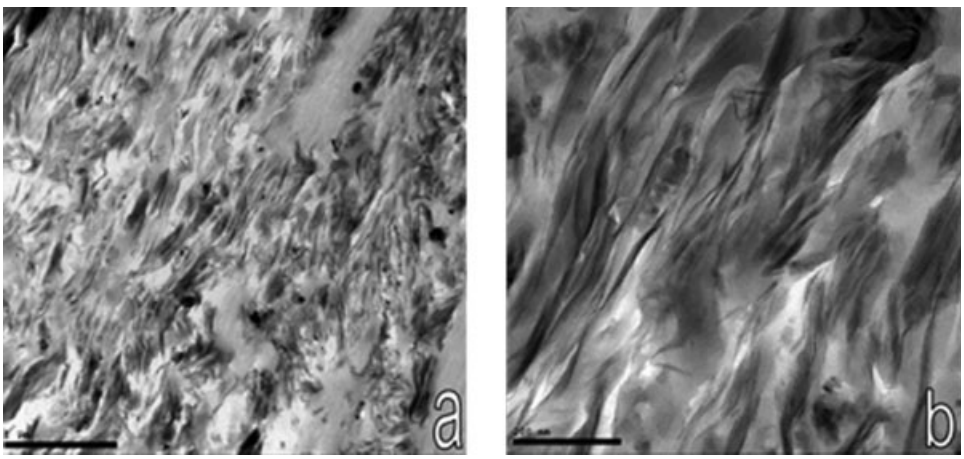

Figure 7 TEM images of UV-cured OMMT/EA nanocomposites at a clay loading of 3 wt %: (a) a low magnification and (b) a high magnification.

There is no obvious diffraction peak at 2θ values ranging from 1 to 10° for the OMMT UV-cured nanocomposites containing 1 or 3 wt % clay. However, the UV-cured EA/OMMT nanocomposite containing 5 wt % clay shows a weak and broad peak at the 2θ value of 4.4°, and the average interlayer *d*-spacing of the clay platelets in the polymer matrix is 2.0 nm, which is the same as the *d*-spacing of the OMMT. It is clear now that exfoliation is possible only when the intragallery polymerization is at least equal to or faster than that of the extragallery polymerization, and in this experiment, exfoliation continued until the extragallery resin turned into a gel.[22] Furthermore, a low clay loading is also required for exfoliation. As the clay loading reaches up to 5 wt %, the clay platelets are more likely to be aggregated. For clay nanocomposites, it is normal for exfoliation to occur at low loadings and intercalation to occur at high loadings.[23–28] In addition, the photodegradation of anchored initiators in the clay will reduce the *d*-spacing of the clay.[29] Therefore, it is not a surprise to see no change or a decrease in the *d*-spacing of the clay for UV-cured EA/OMMT nanocomposites at a high clay loading.

The absence of an XRD peak for nanocomposites containing 1 or 3 wt % clay in EA/OMMT does not necessarily mean exfoliation, as the observed absence of scattering could be due to geometry effects or a lack of sensitivity at the low clay loading. To confirm the structure of EA/OMMT nanocomposites with a clay loading below 3 wt %, TEM experiments were performed. Typical TEM images of samples are shown in Figure 7. It is obvious from the low-magnification image [Fig. 7(a)] that the clay was well dispersed in the UV-cured polymer. At a high magnification, the TEM image [Fig. 7(b)] reveals both very thin isolated clay layers and parallel clay layers on the edge of the clay particles, indicating that a mixture of exfoliated and intercalated structures was present in the nanocomposites.

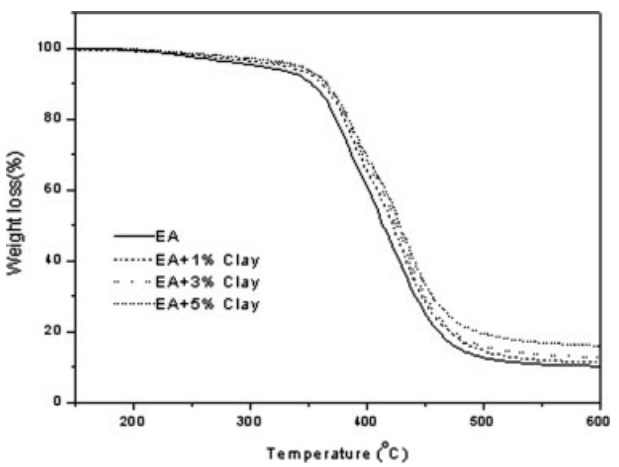

Figure 8 TGA traces obtained from the EA polymer and its OMMT nanocomposites.

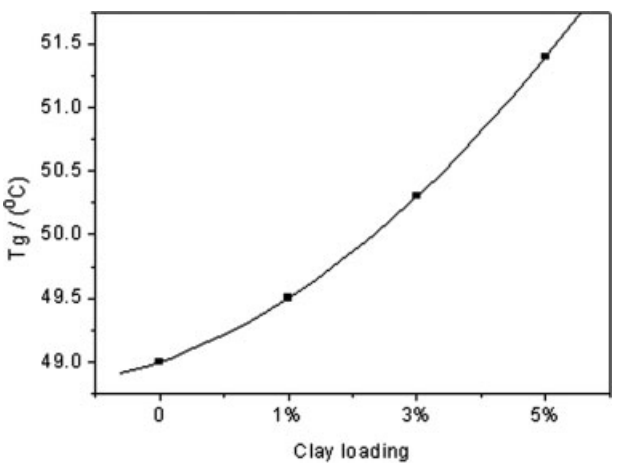

Figure 9 Effect of the clay loading on the T_g values of UV-cured EA/OMMT nanocomposites.

TABLE II
Mechanical Properties of Pure EA and Its Nanocomposites

Material	Tensile strength (MPa)	Elastic modulus (GPa)	Elongation at break (%)
Pure EA	27.0 ± 1.8	1.24 ± 0.3	3.5 ± 0.4
1% clay	33.3 ± 2.2	1.42 ± 0.2	3.2 ± 0.6
3% clay	35.5 ± 2.3	1.57 ± 0.3	2.8 ± 0.3
5% clay	40.2 ± 2.4	2.12 ± 0.4	2.6 ± 0.6

Thermal properties of the EA/MMT UV-cured nanocomposites

High thermal stability is required in processing and applications for polymers in electronics; therefore, TGA and DSC experiments were performed with the samples prepared in this research. TGA traces are shown in Figure 8. The UV-cured EA/OMMT nanocomposites films exhibited improved thermal degradation properties with respect to pure polymer films at a loading of clay even lower than 1%.

Figure 9 shows T_g values for the photocured polymer films obtained from DSC experiments. The polymer films containing MDAB-modified MMT had higher T_g values than the pure polymer films because of the confinement of the polymer chains between the clay layers, which limited segmental motion of the polymer chain.[30]

Mechanical properties of the nanocomposite films

It is well known that filler particles reduce the molecular mobility of polymer chains, resulting in a less flexible material with a higher tensile strength and elastic modulus. This reinforcement effect increases with the volume fraction and dispersion of the filler increasing.[20] As shown in Table II, the tensile strength increases from 27.0 to 40.2 MPa as the content of clay increases to 5 wt %, whereas the elastic modulus also increases from 1.24 to 2.12 GPa. However, the elongation at break decreases from 3.5 to 2.7%. This reduction of the elongation at break is caused by the lowered molecular mobility of the epoxy network induced by the presence of the rigid, immobile clay platelet structure.[20,24,31]

CONCLUSIONS

MDAB, a bifunctional cationic photoinitiator, was used to prepare OMMT and its EA nanocomposites, which could be used in the electronics field. The morphologies of the resulting UV-cured nanocomposites were characterized with XRD and TEM, and the experimental results showed that the OMMT had an intercalated structure and was well-dispersed in the polymer. The overall performance of this material suggests that the current approach using a bifunctional initiator inside the clay galleries is a promising strategy for the preparation of high-performance photocured polymer nanocomposites.

References

1. Cook, W. D. J Polym Sci Part A: Polym Chem 1993, 31, 1053.
2. Decker, C. Prog Polym Sci 1996, 21, 593.
3. Andrzejewska, E. Prog Polym Sci 2001, 26, 605.
4. Pinnavaia, T. J. Science 1983, 220, 365.
5. Decker, C.; Keller, L.; Zahouily, K.; Benfarhi, S. Polymer 2005, 46, 6640.
6. Wang, W. J.; Chen, W. K. J Polym Sci Part B: Polym Phys 2002, 40, 1690.
7. Wu, J.; Lerner, M. M. Chem Mater 1993, 5, 835.
8. Zahouily, K.; Benfarhi, S.; Bendaikha, T.; Baron, J.; Deck, C. Proc Rad Tech Europe Conference 2001, 583.
9. Benfarhi, S.; Decker, C.; Keller, L.; Zahouily, K. Eur Polym J 2004, 40, 493.
10. Yebassa, D.; Balakrishnan, S.; Feresenbet, E.; Raghavan, D.; Start, P. R.; Hudson, S. D. J Polym Sci Part A: Polym Chem 2004, 42, 1310.
11. Uhl, F. M.; Davuluri, P. S.; Wong, S. C.; Webster, D. C. Chem Mater 2004, 16, 1135.
12. Bozena, P.; Slawomir, S.; Beata, J.; Lars-Ake, L.; Jerzy, P. Appl Clay Sci 2004, 25, 221.
13. Uhl, F. M.; Hinderliter, B. R.; Davuluri, P. S.; Croll, S. G.; Wong, S. C.; Webster, D. C. Polym Prepr 2003, 44, 247.
14. Benfarhi, S.; Decker, C.; Keller, L.; Zahouily, K. Eur Polym J 2003, 40, 493.
15. Keller, L.; Decker, C.; Zahouily, K.; Benfarhi, S.; Le Meins, J. M.; Miehe-Brendle, J. Polymer 2004, 45, 7437.
16. Dean, M. K.; Bateman, A. S.; Simons, R. Polymer 2007, 48, 2231.
17. Wang, Y. Y.; Hsieh, T. E. Chem Mater 2005, 17, 3331.
18. Su, S. P.; Wilkie, C. A. J Polym Sci Part A: Polym Chem 2003, 41, 1124.
19. Uhl, F. M.; Davuluri, S. P.; Wong, S. C.; Webster, D. C. Polymer 2004, 45, 6175.
20. Hsiao, S. H.; Liou, G. S.; Chang, L. M. J Appl Polym Sci 2001, 80, 2067.
21. Agag, T.; Koga, T.; Takeichi, T. Polymer 2001, 42, 3399.
22. Park, J. M.; Jana, S. C. Macromolecules 2003, 36, 2758.
23. Uthirakumar, P.; Song, M. K.; Nah, C.; Lee, Y. S. Eur Polym J 2005, 41, 211.
24. Uthirakumar, P.; Nahm, K. S.; Hahn, Y. B.; Lee, Y. S. Eur Polym J 2004, 40, 2437.
25. Uthirakumar, P.; Hahn, Y. B.; Nahm, K. S.; Lee, Y. S. Eur Polym J 2005, 41, 1582.
26. Ranade, A.; D'Souza, N. A.; Gnade, B. Polymer 2002, 43, 3759.
27. Hsiao, S. H.; Liou, G. S.; Chang, L. M. J Appl Polym Sci 2001, 80, 2067.
28. Agag, T.; Koga, T.; Takeichi, T. Polymer 2001, 42, 3399.
29. Fan, X.; Xia, C.; Advincula, R. C. Colloids Surf A 2003, 219, 75.
30. Ogawa, M.; Kuroda, K. Bull Chem Soc Jpn 1997, 70, 2593.
31. Sue, H. J.; Gam, K. T. Chem Mater 2004, 16, 242.